AFRL-VS-HA-TR-2005-1177

The Radiation Environment Impacting DSX Orbit Options

Gregory P. Ginet

6 Dec 2005

AIR FORCE RESEARCH LABORATORY
Space Vehicles Directorate
29 Randolph Rd
AIR FORCE MATERIEL COMMAND
Hanscom AFB, MA 01731-3010

AFRL-VS-HA-TR-2005-1177

When Government drawings, specifications, or other data included in this document are used for any purpose other than Government procurement, this does not in any way obligate the U.S, Government. The fact that the Government formulated or supplied the drawings, specifications, or other data does not license the holder or any other person or corporation; or convey any rights or permission to manufacture, use, or sell any patented invention that may relate to them.

This technical report has been reviewed and is approved for publication.

/ signed /
Gregory P. Ginet, DR-IV
Space Weather Center of Excellence

/ signed /
Joel B. Mozer, Chief
Space Weather Center of Excellence

/ signed /
Robert A. Morris, Chief
Battlespace Environment Division
Space Vehicles Directorate

This report is published in the interest of scientific and technical information exchange and its publication does not constitute the Government's approval or disapproval of its ideas or findings.

This report has been reviewed by the ESC Public Affairs Office (PA) and is releasable to the National Technical Information Service (NTIS).

Qualified requestors may obtain additional copies from the Defense Technical Information Center (DTIC). All other requestors should apply to the National Technical Information Service (NTIS).

If your address has changed, if you with to be removed from the mailing list, or if the addressee is no longer employed by your organization, please notify AFRL/VSIM, 29 Randolph Rd., Hanscom AFB, MA 01731-3010. This will assist us in maintaining a current mailing list.

Do not return copies of this report unless contractual obligations or notices on a specific document require that it be returned.

REPORT DOCUMENTATION PAGE

Form Approved
OMB No. 0704-01-0188

PLEASE DO NOT RETURN YOUR FORM TO THE ABOVE ADDRESS.

1. REPORT DATE *(DD-MM-YYYY)*	2. REPORT TYPE	3. DATES COVERED *(From - To)*
06-12-2005	Scientific, Interim	

4. TITLE AND SUBTITLE
The Radiation Environment Impacting DSX Orbit Options

5a. CONTRACT NUMBER

5b. GRANT NUMBER

5c. PROGRAM ELEMENT NUMBER
62601F

6. AUTHORS
Gregory P. Ginet

5d. PROJECT NUMBER
1010

5e. TASK NUMBER
RR

5f. WORK UNIT NUMBER
A1

7. PERFORMING ORGANIZATION NAME(S) AND ADDRESS(ES)
Air Force Research Laboratory /VSBX
29 Randolph Road
Hanscom AFB, MA 01731-3010

8. PERFORMING ORGANIZATION REPORT NUMBER
AFRL-VS-HA-TR-2005-1177

9. SPONSORING/MONITORING AGENCY NAME(S) AND ADDRESS(ES)

10. SPONSOR/MONITOR'S ACRONYM(S)
AFRL/VSBX

11. SPONSOR/MONITOR'S REPORT NUMBER(S)

12. DISTRIBUTION/AVAILABILITY STATEMENT
Approved for public release; distribution unlimited.

13. SUPPLEMENTARY NOTES

14. ABSTRACT

The Air Force Research Laboratory plans.to fly the Demonstrations and Science Experiment (DSX) in a medium Earth orbit (MEO) to study wave-particle interaction in the Very Low Frequency (VLF) regime and (b) map the energetic particle and plasma environment in the middle magnetosphere. Since the initial DSX planning, interest has surfaced in mapping the energetic particle environment of the inner belt inside the MEO regime. The question arises whether the DSX orbit could be modified to accomplish sufficient inner-belt mapping without compromising the primary DSX science missions. It is concluded that the optimum orbit to map the L, B/B0 region relevant to the inner belt orbits while maintaining the capability of DSX to map and carry out experiments in the slot region is a 540 x 12000 km orbit with 28 degrees *or less* of inclination. The energetic electrons in the horns of the outer belt will be missed; however, this population has been much better characterized by existing data sets than have the populations in the inner magnetosphere. Doses for the recommended orbit are approximately an order of magnitude higher than for the nominal DSX orbit, but lower by a factor of approximately two than the worst inner belt orbit considered.

15. SUBJECT TERMS

Radiation belts	Medium-earth orbit
Space environment	Demonstration and Science Experiment (DSX)

16. SECURITY CLASSIFICATION OF:			17. LIMITATION OF ABSTRACT	18. NUMBER OF PAGES	19a. NAME OF RESPONSIBLE PERSON
a. REPORT	b. ABSTRACT	c. THIS PAGE			Gregory P. Ginet
UNCL	UNCL	UNCL	UNL		19B. TELEPHONE NUMBER *(Include area code)* (781) 377-3974

Contents

Illustrations

Illustrations (Cont.)

Tables

The Radiation Environment Impacting DSX Orbit Options

1. INTRODUCTION

The Air Force Research Laboratory (AFRL) plans to fly the Demonstrations and Science Experiment (DSX) satellite in a medium Earth orbit (MEO) to (a) study wave-particle interactions in the Very Low Frequency (VLF) regime relevant for radiation belt dynamics and (b) map the energetic particle and space plasma environment in the largely unexplored middle magnetosphere. To achieve the mission objectives the DSX orbit was nominally chosen to be 6,000 km x 12,000 km with 28 degree inclination.

Since the initial DSX planning, interest has surfaced in mapping the energetic particle environment of the inner-belt inside the MEO regime. The question arises as to whether the DSX orbit could be modified to accomplish sufficient inner-belt mapping without compromising the primary DSX science missions. It is the purpose of this report to provide the environmental analysis needed to answer such a question (Sec 2) and offer recommendations (Sec 3).

2. ANALYSIS

A set of orbits has been selected for analysis (Table 1) with inclinations of 28 degrees and 63 degrees to include the nominal DSX orbit (1) and variations that only sample the inner belt (orbits 9 and 10). With the exception of orbit 10, all orbits will be initialized with the local time of maximum latitude (LTML) equal to 18:00 and the local time of apogee (LTA) equal to 12:00.

Variations of the proton fluence for different values of LTA and LTML were examined for the DSX (1) and inner belt (9) orbits. Little difference was discovered for the DSX orbit (<10%) while differences greater than an order of magnitude were uncovered for the inner belt orbits. For this reason two different sets of LTML and LTA were considered for the inner belt orbit spanning the range from the approximate minimum (9) to maximum (10) of inner belt radiation exposure. Figures 1a and 1b illustrate the orbit paths in the context of the active time inner proton belt and average outer zone electron belts as determined from the CRRESPRO and CRRESELE models, respectively. The passage of orbit 10 through the heart of the inner belt (always existing) while the passage of orbit 9 only through the middle belt (only existing in active times) and largely missing the inner belt due to the different orientation of the orbit plane and location of perigee, is apparent.

Table 1. Orbital Parameters Specified as Inclination, Perigee, Apogee, Local Time of Apogee and Local Time of Maximum Latitude.

Orbit #	Incl (deg)	Perigee(km)	Apogee (km)	LT of Apogee	LT of Max Lat
1	28.0	6000	12000	12:00	18:00
2	28.0	4000	12000	12:00	18:00
3	28.0	2000	12000	12:00	18:00
4	28.0	500	12000	12:00	18:00
5	63.0	6000	12000	12:00	18:00
6	63.0	4000	12000	12:00	18:00
7	63.0	2000	12000	12:00	18:00
8	63.0	500	12000	12:00	18:00
9	63.0	540	7840	12:00	18:00
10	63.0	540	7840	12:00	12:00

To estimate the relative severity of the space particle environment, each orbit will be run for approximately one year (12:00 UT 01 Jan 2002 – 12:00 UT 31 Dec 2002) through a series of space environment models to include the standard NASA AP8 /AE8, the Air Force CRRES suite, and the JPL 1991 model for solar particle events. The spread in values predicted by the model suite for a given quantity (e.g. 36.3 MeV proton fluence in Figure 2b) can be viewed as error bars representing variations due to space weather as well as uncertainties in the models themselves.

The degree to which an appropriately instrumented satellite can map the inner radiation belt and MEO regimes will be assessed by examining orbit coverage in the (L, B/B0) magnetic coordinate space. This is a natural space for mapping the belts because trapped energetic particles spiral along magnetic field lines, bouncing between mirror points of equal magnetic magnitude in the southern and northern hemispheres while at the same time drifting around the planet on an azimuthal shell of field lines with identical properties. Shells are labeled by the distance from the center of the Earth to a given magnetic field line along the magnetic equator (L). Locations along a magnetic field line are denoted by the ratio of the strength of the local magnetic field (B) to the strength of the magnetic field at the magnetic equator (B0). Energetic particle populations in a given L-shell can also be quantified by their distributions in equatorial pitch-angle, defined as the angle between the velocity parallel and perpendicular to the magnetic field when the particle crosses the magnetic equator (0 degrees equals entirely parallel velocity). Particles with smaller pitch-angles will travel further down the field lines before mirroring and thus reach a higher value of B/B0 since the field strength is weakest at the magnetic equator and increases along the field line as the Earth is approached. Distributions in the (L, B/B0) coordinates are tagged to the highest value of B/B0 a particle reaches.

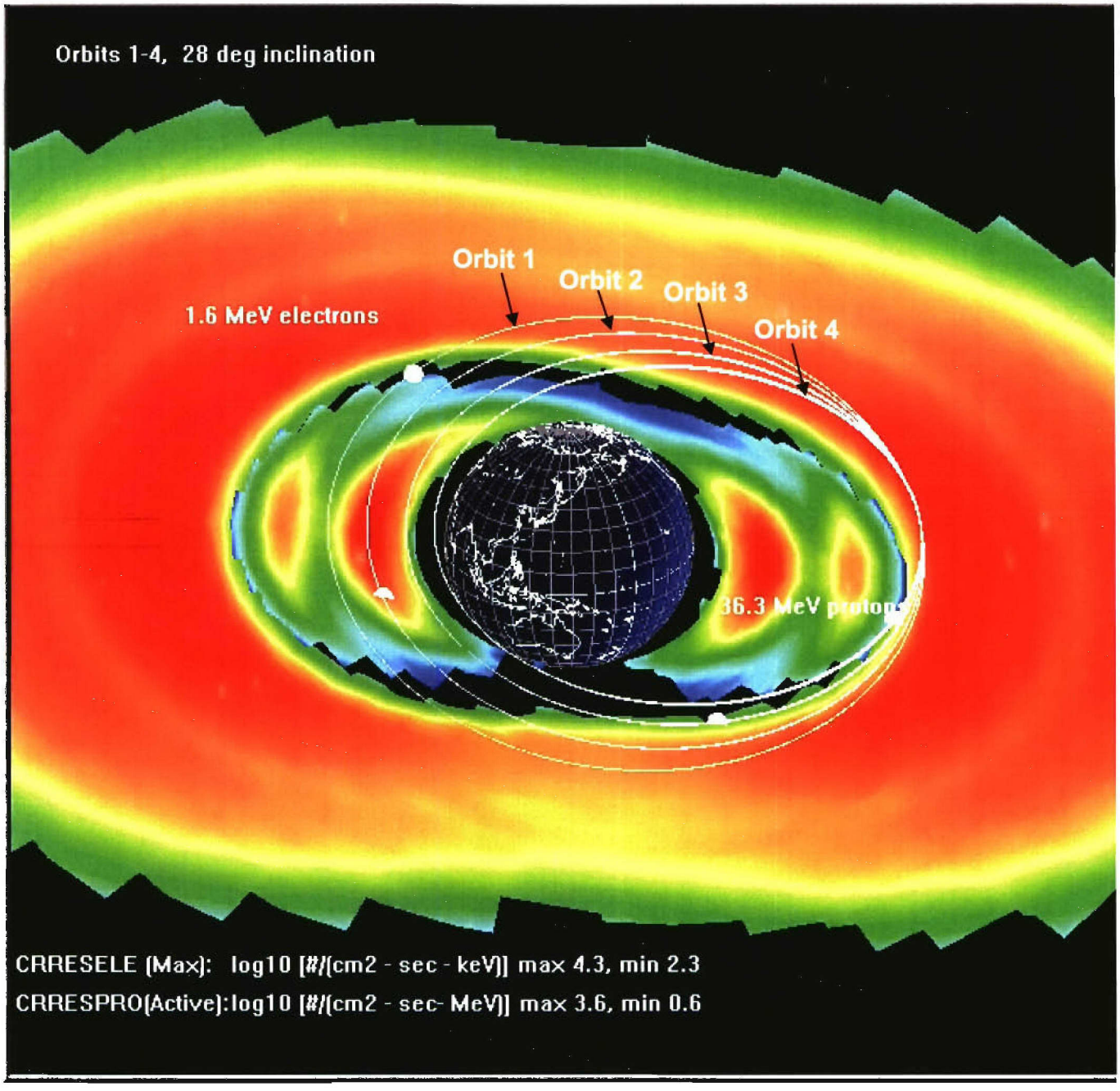

Figure 1a. Orbits 1-4 With Orbit-Plane (28 degree) Slices of the Trapped 1.6 MeV Electron and 36.3 MeV Proton Fluxes From the CRRESELE (MAX) and CRRESPRO (Active) Models, Respectively. The coloring indicates the intensity of the differential flux.

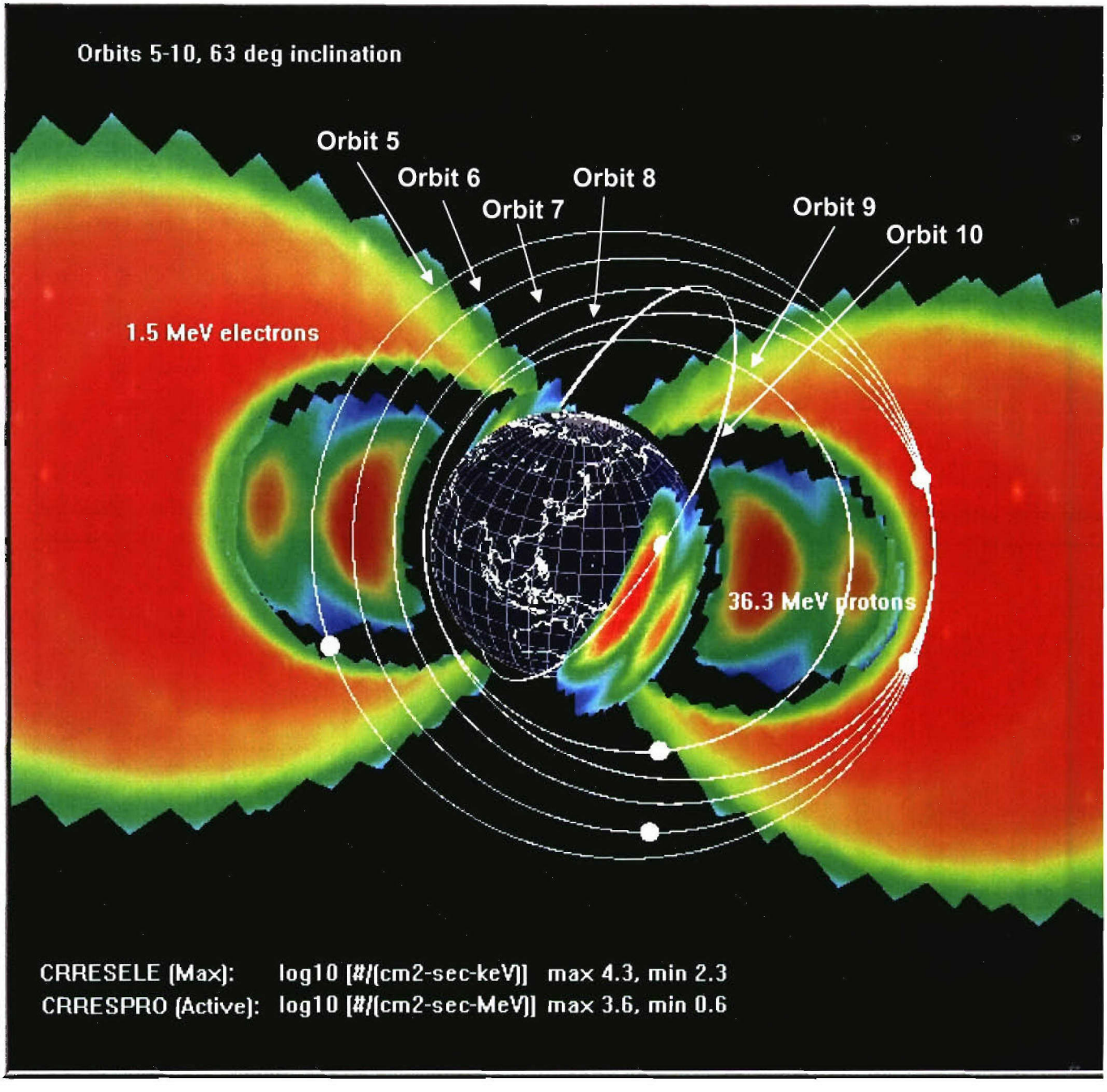

Figure 1b. Orbits 5-10 With Orbit-Plane (63 degree) Slices of the Trapped 1.6 MeV Electron and 36.3 MeV Proton Fluxes From the CRRESELE (MAX) and CRRESPRO (Active) Models, Respectively. Only the CRRESPRO Active is shown for the plane of orbit 10. Coloring indicates the intensity of the differential flux.

An important consequence of the trapped particle motion is that if the entire pitch angle distribution is measured near the magnetic equator then the entire space represented by a magnetic field line can be mapped, thus turning an *in-situ* spacecraft measurement into an estimate of a global distribution. This can be accomplished, for example, by a low inclination satellite carrying a magnetometer and particle detectors with sufficient local angle of arrival resolution and range. Inside L ~ 4.0, models of the global magnetic field are sufficiently accurate to perform the mapping given a magnetic field measurement on the spacecraft. Detectors in higher inclination orbits will never be able to sample the distribution mirroring below them where often the bulk of the particles lie waiting to be scattered to higher B/B0 values by magnetospheric processes.

2.1. Protons

To estimate exposure to trapped energetic protons the orbits were run through the AP8 (Vette, 1991) as implemented in the NASAPRO modules of AF-GEOSpace Version 2.0 (Hilmer 2001) and CRRESPRO (Gussenhoven, et al., 1993; Meffert and Gussenhoven, 1994; Hilmer, 2001) models. Differential energy fluences/year [#/(cm2-MeV-yr)] were calculated for protons of 1.5 MeV, 36.3 MeV and 81.3 MeV. Integral energy fluence [#/(cm2 – yr)] was computed for > 10 MeV protons. The NASA models represent both solar maximum (AP8MAX) and solar minimum (AP8MIN) conditions while CRRESPRO has representations of "quiet" and "active" conditions. CRRESPRO was constructed from CRRES satellite data (Jul 1990 – Oct 1991) and the quiet/active models represent that state of the radiation belts before/after a new, long-lived radiation belt between the inner-belt and the outer zone was created during the great magnetic storm of March 1991. Fluence values from all four models for the four energy regimes discussed are presented in Table 2 (CRRESPRO), Table 3 (NASAPRO) and Figures 2a-d. Both models have reasonable coverage of the orbit space as is apparent from Figure 1.

Proton fluence due to the transient solar energetic proton (SEP) events can be estimated using the JPL 1991 Interplanetary Fluence Model (Feynman, et al., 1993). At the 95% and 70% confidence levels the fluence values for a one-year mission at solar maximum are 2.64e+11 and 5.0e+10 [#/(cm2 – yr)], respectively. These can be compared directly to the trapped particle fluence values shown in Table 2 and Figure 2d. The JPL model values are overestimates because they are calculated for (a) interplanetary space, not the Earth-bound orbit regime of DSX shielded from SEPs to a non-trivial degree by the geomagnetic field, and (b) a year period around solar maximum, not a year period during the rising phase of the solar cycle in which DSX will be launched (2007-2009 timeframe).

For the lower energy protons, as exemplified by the 1.5 MeV fluence shown in Figure 2a, the nominal DSX orbit is the more severe environment because the radial peak of the lower energy proton belt is in the L shell = 2 –3 range. As the energy increases the radial peak moves inward and the maximum fluence is experienced by those orbits spending the most time in the L shell = 1.5 – 1.8 near the magnetic equator, i.e. orbits 2, 3 and 10 (Figures 2b-d). The wide variation in fluence experienced by the inner belt orbit with different choices of LTML can be seen by comparing orbits 9 and 10.

Table 2. Proton Fluences for Orbits 1-10 Computed by the CRRESPRO Active and Quiet Models.

	Fluence/yr [# / (cm^2 - MeV - yr)]						[# / (cm^2 - yr)]	
	1.5 MeV		36.3 MeV		81.3 MeV		> 10 MeV (2)	
Orbit #	Quiet	Active	Quiet	Active	Quiet	Active	Quiet	Active
1	8.27E+13	8.66E+13	1.86E+08	1.55E+09	4.40E+07	5.10E+07	5.47E+10	2.67E+11
2	6.29E+13	7.04E+13	3.92E+09	4.37E+09	5.67E+08	5.11E+08	5.63E+11	6.16E+11
3	6.35E+13	6.33E+13	5.10E+09	5.56E+09	1.48E+09	1.38E+09	5.79E+11	6.37E+11
4	6.34E+13	6.25E+13	3.44E+09	3.97E+09	9.31E+08	8.68E+08	4.08E+11	4.70E+11
5	3.10E+13	3.23E+13	1.58E+08	2.46E+08	2.93E+07	2.35E+07	3.97E+10	1.33E+11
6	3.22E+13	2.95E+13	3.19E+09	2.76E+09	4.75E+08	4.27E+08	4.15E+11	3.42E+11
7	3.93E+13	3.49E+13	1.15E+09	1.10E+09	6.07E+08	5.80E+08	8.87E+10	8.52E+10
8	4.73E+13	4.14E+13	1.65E+08	1.71E+08	5.57E+07	5.24E+07	1.81E+10	2.04E+10
9	3.30E+13	4.94E+13	2.90E+08	2.34E+09	9.51E+07	1.22E+08	5.03E+10	2.33E+11
10	2.53E+12	3.92E+12	7.58E+09	7.12E+09	2.24E+09	2.09E+09	7.94E+11	7.38E+11

2.2. Electrons

Energetic electron environments were estimated using the AE8 (Vette, 1991) as implemented in the NASAELE module of AF-GEOSpace Version 2.0 (Hilmer, 2001) and CRRESELE (Brautigam, et al., 1992; Brautigam and Bell, 1995; Hilmer, 2001) models. Differential energy fluences/year were calculated for electrons of 0.65 MeV, 1.6 MeV and 5.75 MeV. Integral energy fluence [#/(cm2 – yr)] was computed for > 1.25 MeV. The NASA models represent both solar maximum (AE8MAX) and solar minimum (AE8MIN) conditions. CRRESELE comprises a sequence of 6 models corresponding to six different ranges of the 15 day average of the geomagnetic Ap index (Ap-15). In addition there are two models capturing the maximum and average values measured at each location during the CRRES mission regardless of the Ap-15 value. These latter CRRESELE models are used in this study. Fluence values from all four models for the four energy regimes discussed are presented in Table 4 (CRRESELE), Table 5, (NASAELE) and Figures 3a-3d. Both models have reasonable coverage of the orbit space as is apparent from Figure 1. For orbits 8 and 10 perigees of 540 km and 600 km were used, respectively, to avoid orbit-integrator convergence problems in the CRRESELE code. The difference in integrated fluences is negligible.

Table 3. Proton Fluences for Orbits 1-10 Computed by the NASAPRO AP8MAX and AP8MIN Models.

	Fluence/yr [# / (cm^2 - MeV - yr)]						[# / (cm^2 - yr)]	
	1.5 MeV		36.3 MeV		81.3 MeV		> 10 MeV (2)	
Orbit #	AP8MIN	AP8MAX	AP8MIN	AP8MAX	AP8MIN	AP8MAX	AP8MIN	AP8MAX
1	2.47E+14	2.47E+14	6.42E+08	6.42E+08	2.65E+07	2.65E+07	6.07E+11	6.07E+11
2	2.12E+14	2.12E+14	1.63E+09	1.63E+09	1.64E+08	1.64E+08	1.07E+12	1.06E+12
3	1.95E+14	1.95E+14	2.24E+09	2.23E+09	4.71E+08	4.63E+08	9.70E+11	9.67E+11
4	1.96E+14	1.96E+14	1.59E+09	1.57E+09	3.26E+08	3.12E+08	7.51E+11	7.48E+11
5	1.22E+14	1.22E+14	3.90E+08	3.89E+08	2.06E+07	2.06E+07	3.27E+11	3.27E+11
6	1.31E+14	1.31E+14	8.53E+08	8.52E+08	1.21E+08	1.21E+08	4.37E+11	4.37E+11
7	1.55E+14	1.55E+14	5.85E+08	5.73E+08	2.28E+08	2.17E+08	1.04E+11	1.01E+11
8	1.80E+14	1.80E+14	8.23E+07	7.64E+07	2.69E+07	2.27E+07	4.08E+10	4.01E+10
9	7.14E+13	7.14E+13	4.81E+08	4.72E+08	4.62E+07	4.01E+07	4.27E+11	4.26E+11
10	8.12E+12	8.12E+12	2.92E+09	2.90E+09	6.97E+08	6.85E+08	9.42E+11	9.38E+11

The DSX orbits 1-8 have approximately equivalent fluences, which are significantly greater than those estimated for the inner belt orbits 9-10. This is due to the 12000 km apogee which puts the DSX orbits deeper into the heart of the outer zone electron belt (Figure 1).

2.3. Radiation Dose

To compare radiation doses for the study orbit the CRRESRAD model was used (Gussenhoven, et al., 1992; Kerns and Gussenhoven, 1992; Hilmer, 2001). CRRESRAD was constructed from dosimeter measurements made aboard the CRRES satellite (Jul 1990 – Oct 1991) and, similar to the CRRESPRO model, is divided into quiet/active models representing data taken before/after the great geomagnetic storm of March 1991 which formed a new radiation belt within the slot region. Doses were measured behind four hemispheres of Aluminum with shielding thicknesses of 2.1 mm, 5.91 mm, 11.6 mm, and 22.5 mm. Table 5 and Figure 4 present the quiet and active time dose estimates in units of Rads/silicon per year. Also given is the percentage of time that the orbit, run for a full year, lies outside the orbit domain. Unlike measurements of energetic protons and electrons which can be globally mapped (as discussed at the beginning of this section) dose measurements are purely local and the coverage provided by the CRRESRAD model is limited to the space sampled by the CRRES satellite. Figure 5

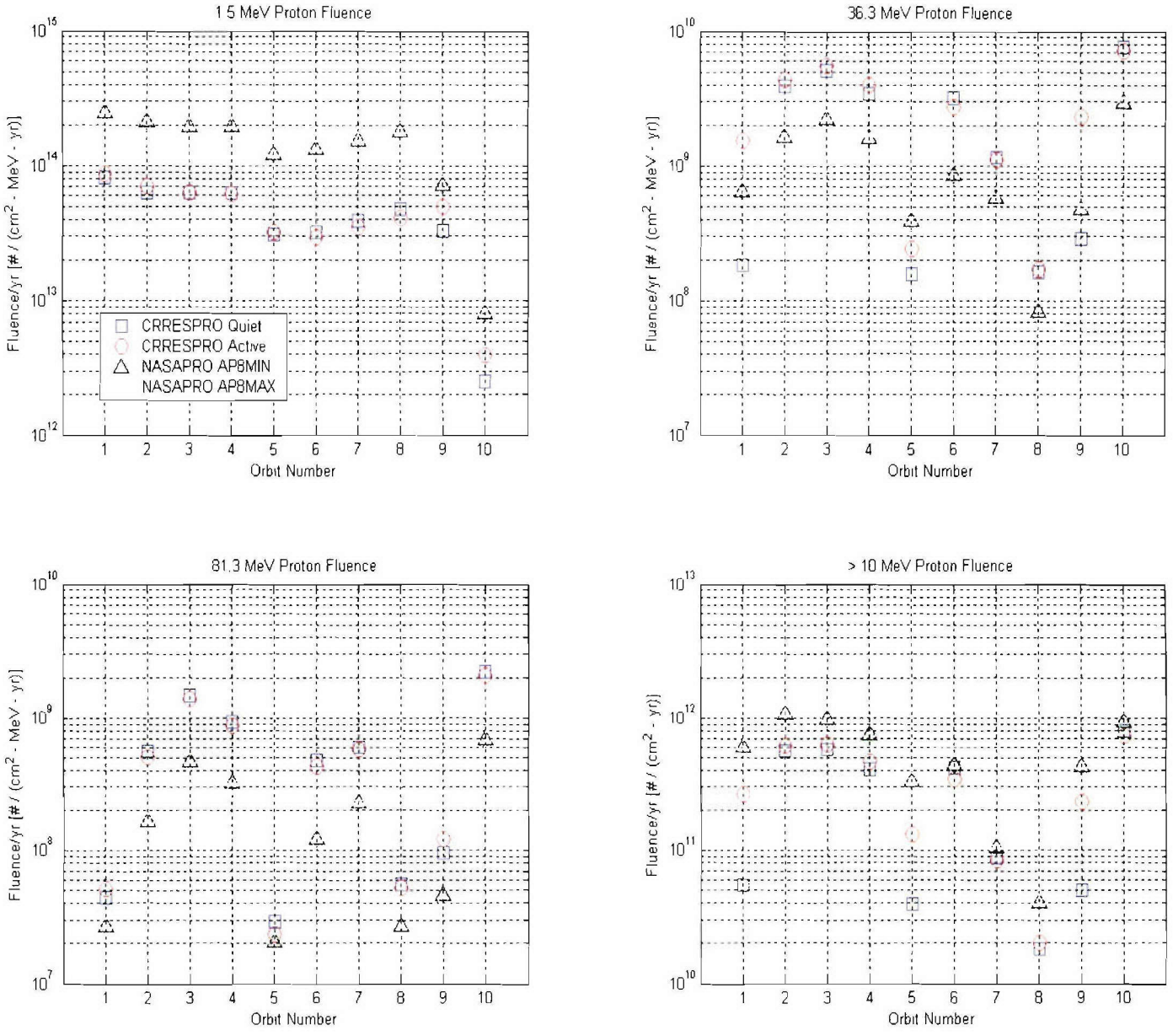

Figure 2. Proton Fluences at (a) 1.5 MeV, (b) 36.3 MeV, (c) 81.3 MeV, and (d) > 10 MeV as Determined by the NASAPRO and CRRESPRO Models for Orbits 1-10.

Table 4. Electron Fluences for Orbits 1-10 Computed by the CRRESELE Average and Maximum Models. Orbits 8 and 10 were computed using 540 km and 600 km for perigee, respectively, instead of the nominal values.

	Fluence/yr [# / (cm^2 - keV - yr)]						[# / (cm^2 - yr)]	
	0.65 MeV		1.6 MeV		5.75 MeV		> 1.25 MeV (2)	
Orbit #	Ave	Max	Ave	Max	Ave	Max	Ave	Max
1	2.40E+11	1.96E+12	1.65E+10	2.21E+11	3.69E+06	1.42E+08	9.63E+12	1.29E+14
2	2.11E+11	1.70E+12	1.46E+10	1.94E+11	3.19E+06	1.23E+08	8.53E+12	1.14E+14
3	1.95E+11	1.57E+12	1.36E+10	1.81E+11	2.97E+06	1.15E+08	7.93E+12	1.06E+14
4	1.90E+11	1.54E+12	1.33E+10	1.77E+11	2.97E+06	1.15E+08	7.78E+12	1.04E+14
5	1.82E+11	1.19E+12	1.42E+10	1.88E+11	1.78E+06	7.31E+07	8.17E+12	1.09E+14
6	1.91E+11	1.28E+12	1.51E+10	2.02E+11	2.01E+06	8.29E+07	8.71E+12	1.17E+14
7	2.07E+11	1.45E+12	1.63E+10	2.18E+11	2.43E+06	1.00E+08	9.41E+12	1.27E+14
8	2.20E+11	1.63E+12	1.68E+10	2.29E+11	2.89E+06	1.18E+08	9.77E+12	1.33E+14
9	1.01E+11	7.07E+11	5.24E+09	6.80E+10	6.80E+05	2.44E+07	2.94E+12	3.88E+13
10	6.92E+10	4.12E+11	3.72E+09	4.95E+10	2.47E+05	9.47E+06	2.07E+12	2.80E+13

displays the active time dose behind 11.6 mm of Al in L, B/B0 coordinates illustrating the range covered by the CRRESRAD model. Two days of trajectory for orbits 1, 5 and 10 are overlayed in Figures 5a, 5b, and 5c. Certainly CRRESRAD provides an underestimate for the dosage received but by a factor much less than that computed by correcting for the relative time spent out of the model range (Table 6) assuming a uniform dose distribution given by the Table 5 values.

Dose estimates computed with the quiet time model fall into two groups: high (orbits 2-4, 6,7 and 9) low (orbits 1, 5, 8 and 10). The low dose orbits all have low exposure to the inner zone protons by either having perigee above (orbits 1 and 5) or missing the belt by 'threading the donut', i.e. crossing the belt altitudes at relatively high latitudes devoid of trapped particles. High dose orbits all hit the inner belt region with the highest dose accumulated in the inner belt orbit (10) going through the center twice per revolution. A factor of > 20 exists between the dose estimated for the inner belt orbits 9 and 10 behind 11.6 mil Al illustrating the large effect of choosing different values of LTML.

Dose estimates computed with the quiet time model fall into two groups: high (orbits 2-4, 6,7 and 9) low (orbits 1, 5, 8 and 10). The low dose orbits all have low exposure to the

Table 5. Electron Fluences for Orbits 1-10 Computed by the NASAELE AE8MAX and AE8MIN Models. Orbits 8 and 10 were computed using 540 km and 600 km for perigee, respectively, instead of the nominal values.

	Fluence/yr [# / (cm^2 - keV - yr)]						[# / (cm^2 - yr)]	
	0.65 MeV		1.6 MeV		5.75 MeV		> 1.25 MeV (2)	
Orbit #	AE8MIN	AE8MAX	AE8MIN	AE8MAX	AE8MIN	AE8MAX	AE8MIN	AE8MAX
1	2.90E+10	1.09E+11	5.16E+09	1.52E+10	9.51E+06	1.08E+07	4.52E+12	1.36E+13
2	2.57E+10	9.62E+10	4.63E+09	1.36E+10	8.42E+06	9.54E+06	4.07E+12	1.22E+13
3	2.43E+10	9.03E+10	4.37E+09	1.28E+10	7.89E+06	8.95E+06	3.84E+12	1.15E+13
4	2.35E+10	8.86E+10	4.25E+09	1.26E+10	7.78E+06	8.84E+06	8.74E+12	1.13E+13
5	3.10E+10	8.32E+10	5.22E+09	1.31E+10	7.66E+06	8.47E+06	4.50E+12	1.16E+13
6	3.02E+10	8.50E+10	5.19E+09	1.36E+10	8.43E+06	9.37E+06	4.50E+12	1.21E+13
7	2.90E+10	8.82E+10	5.09E+09	1.42E+10	9.29E+06	1.04E+07	4.45E+12	1.27E+13
8	2.76E+10	9.01E+10	4.87E+09	1.43E+10	9.64E+06	1.10E+07	4.27E+12	1.28E+13
9	6.81E+09	2.08E+10	1.09E+09	2.47E+09	1.03E+06	1.14E+06	9.11E+11	2.16E+12
10	7.97E+09	1.55E+10	1.16E+09	2.13E+09	6.53E+05	6.98E+05	9.47E+11	1.80E+12

inner zone protons by either having perigee above (orbits 1 and 5) or missing the belt by 'threading the donut', i.e. crossing the belt altitudes at relatively high latitudes devoid of trapped particles. High dose orbits all hit the inner belt region with the highest dose accumulated in the inner belt orbit (10) going through the center twice per revolution. A factor of > 20 exists between the dose estimated for the inner belt orbits 9 and 10 behind 11.6 mil Al illustrating the large effect of choosing different values of LTML.

In active times the doses jump for all orbits due to the presence of the middle belt. The lowest doses are accumulated by the higher inclination

Medium Earth orbits (5-8) which intersect the middle belt at higher latitudes and, with a more distant perigee, spend less time in the inner and outer belt regions than do the inner belt orbits. Long-lived middle belts are a relatively rare occurrence, estimated to happen roughly once per solar cycle (Bell, et al., 1997). However, given the huge increase in dose observed by some MEO orbits (e.g. > 40 for the inner belt #9 orbit behind 11.6 mil Al) the effects could be devastating to systems designed for quiet times. Furthermore, middle belts of lesser magnitude and lifetime than that formed by the March 1991 storm occur much more frequently during a solar cycle and cause substantial dose deviations from those predicted by the CRRES quiet time or dose estimates based on the NASA AP models.

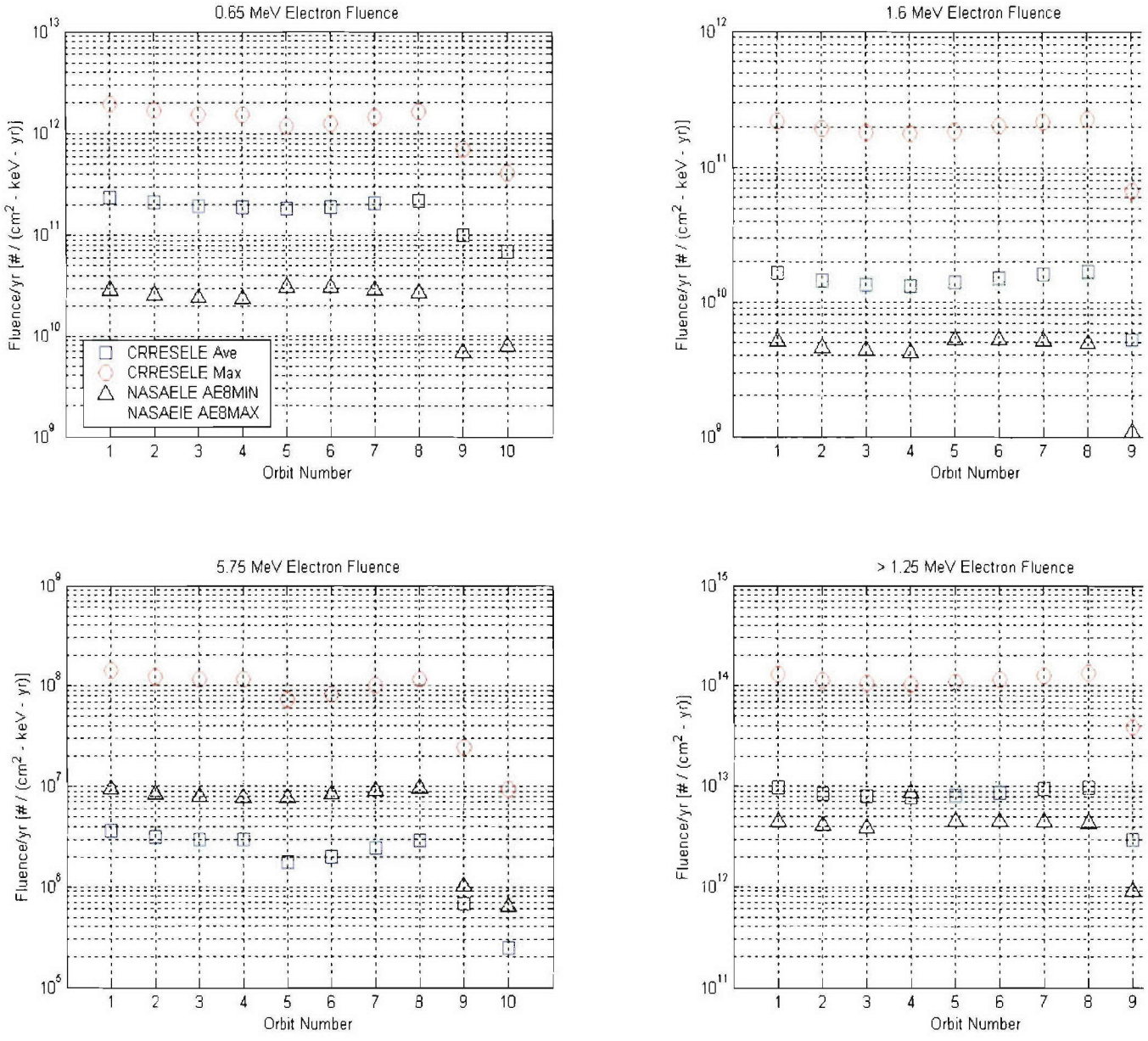

Figure 3. Electron Fluences at (a) 0.65 MeV, (b) 1.6 MeV, (c) 5.75 MeV, and (d) > 1.25 MeV as Determined by the NASAELE and CRRESELE Models for Orbits 1-10.

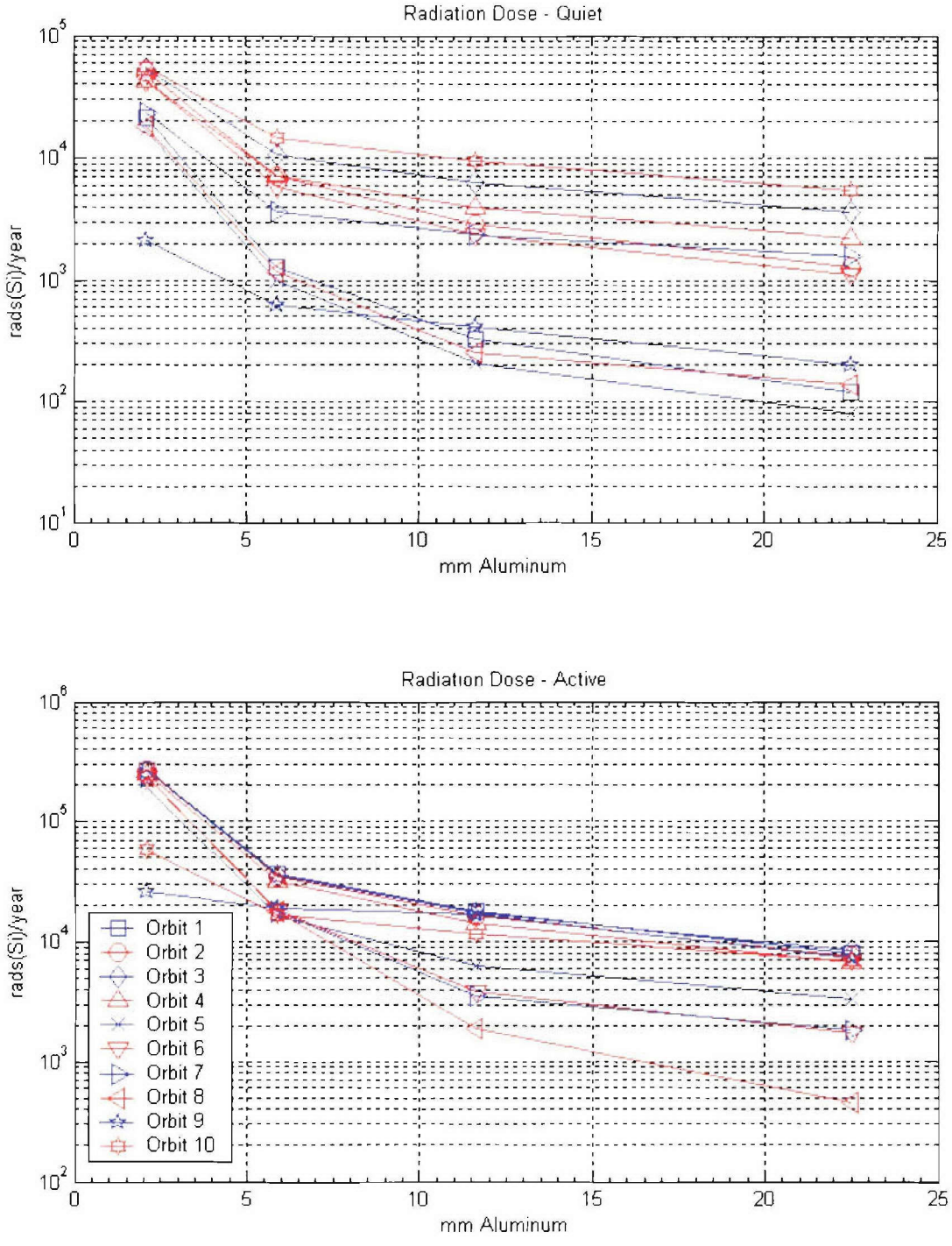

Figure 4. Radiation Doses Behind 2.10 mm, 5.91 mm, 11.6 mm, and 22.5 mm Aluminum as Determined for Orbits 1-10 by the CRRESRAD Quiet (a) and Active (b) Models. Note the change in y-axis scale between (a) and (b).

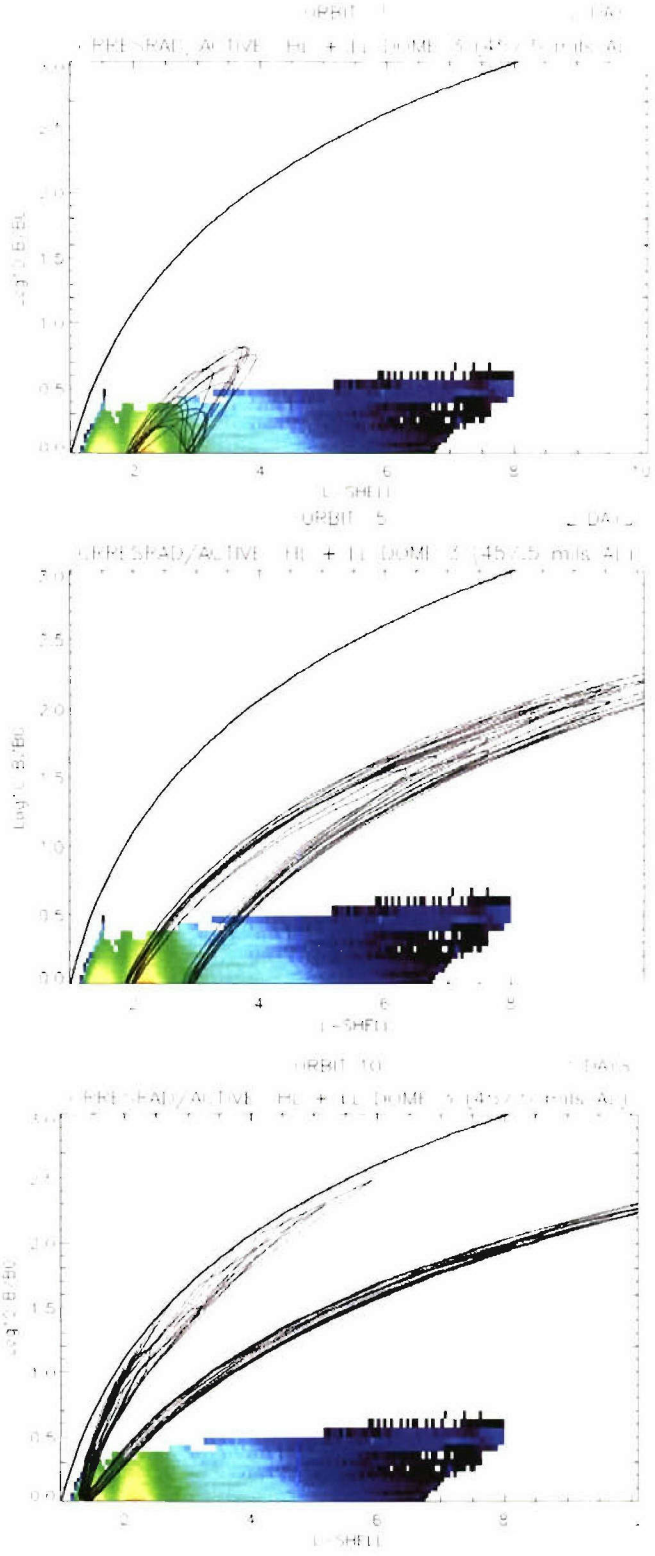

Figure 5. Dose Behind 457.5 mils (11.6 mm) as Determined by the CRRESRAD Active Models Shown in (L, B/B0) Coordinates. Two days of orbit path is shown for orbits (a) 1, (b) 5 and (c) 10. The thick solid line represents the surface of the Earth.

Table 6. Radiation Dose Behind Several Aluminum Shielding Thicknesses for Orbits 1-10 Computed by the CRRESRAD Quiet and Active Models. Percentage of time that the study orbit is out of the model domain is also given.

	Total Dose [rads silicon/yr]								
	2.10 mm Al		5.91 mm Al		11.6 mm Al		22.5 mm Al		
Orbit #	Quiet	Active	Quiet	Active	Quiet	Active	Quiet	Active	% Out
1	2.10E+04	2.70E+05	1.29E+03	3.62E+04	3.29E+02	1.79E+04	1.20E+02	8.05E+03	2.3
2	5.09E+04	2.70E+05	6.97E+03	3.51E+04	2.92E+03	1.62E+04	1.27E+03	7.50E+03	2.2
3	5.40E+04	2.60E+05	1.05E+04	3.58E+04	6.28E+03	1.71E+04	3.60E+03	8.53E+03	2.0
4	4.20E+04	2.50E+05	7.14E+03	3.16E+04	3.99E+03	1.41E+04	2.23E+03	6.69E+03	2.0
5	1.70E+04	1.90E+05	9.78E+02	1.62E+04	2.06E+02	6.30E+03	7.96E+01	3.31E+03	48.0
6	4.30E+04	2.30E+05	5.80E+03	1.83E+04	2.38E+03	3.90E+03	1.10E+03	1.73E+03	45.9
7	2.30E+04	2.30E+05	3.60E+03	1.80E+04	2.38E+03	3.56E+03	1.55E+03	1.81E+03	42.6
8	1.80E+04	2.30E+05	1.16E+03	1.79E+04	2.52E+02	1.88E+03	1.39E+02	4.61E+02	39.6
9	2.10E+03	2.60E+04	6.21E+02	1.88E+04	4.13E+02	1.69E+04	2.02E+02	7.34E+03	42.7
10	5.54E+04	5.89E+04	1.47E+04	1.66E+04	9.33E+03	1.14E+04	5.44E+03	6.89E+03	52.8

2.4. Coverage of L, B/B0

Orbit coverage of L, B/B0 space is illustrated in Figures 6-10 for orbits 1, 4, 5, 9 and 10, respectively. In the top part of each figure (a) two days of orbit path are plotted together with the relative intensities of the 36.3 MeV protons and 1.6 MeV electrons as predicted by the CRRESPRO active and CRRESELE maximum models. The lower portion of each figure (b) shows the dwell time computed from a year's integrated orbit path. At any point along the orbit path a well-instrumented satellite will be able to map the particle distribution along a vertical line in B/B0 from the orbit point up to the dark solid line representing the surface of the Earth.

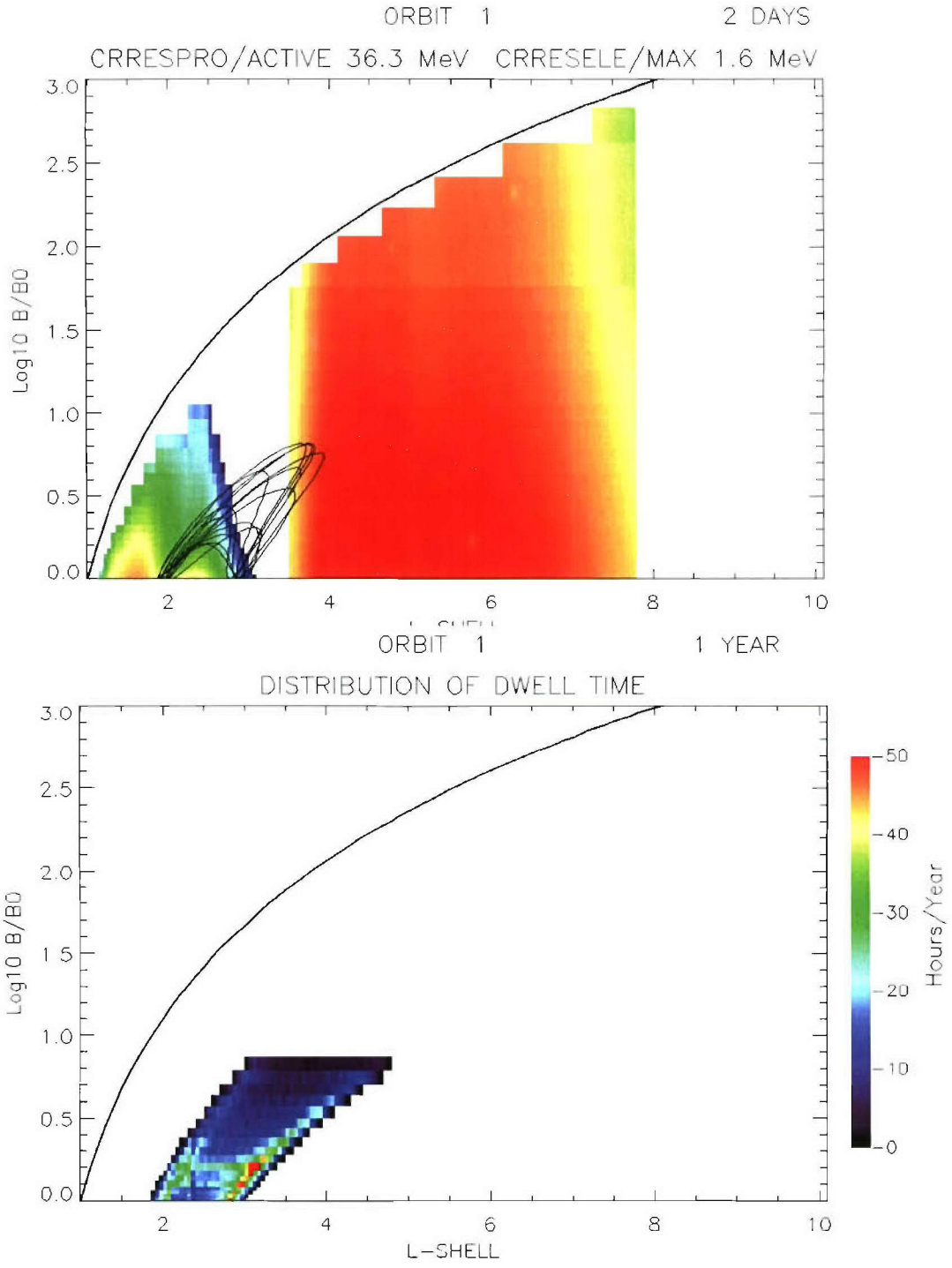

Figure 6. (a) Two Days of Orbit 1 Path (thin solid line) in (L, B/B0) Coordinates Overlayed on the Relative Flux Intensity Distribution of 1.6 MeV Electrons and 36.3 MeV Protons as Determined by the CRRES Models. (b) Dwell time in (L, B/B0) for a Year's Orbit Path. The thick solid line represents the surface of the Earth.

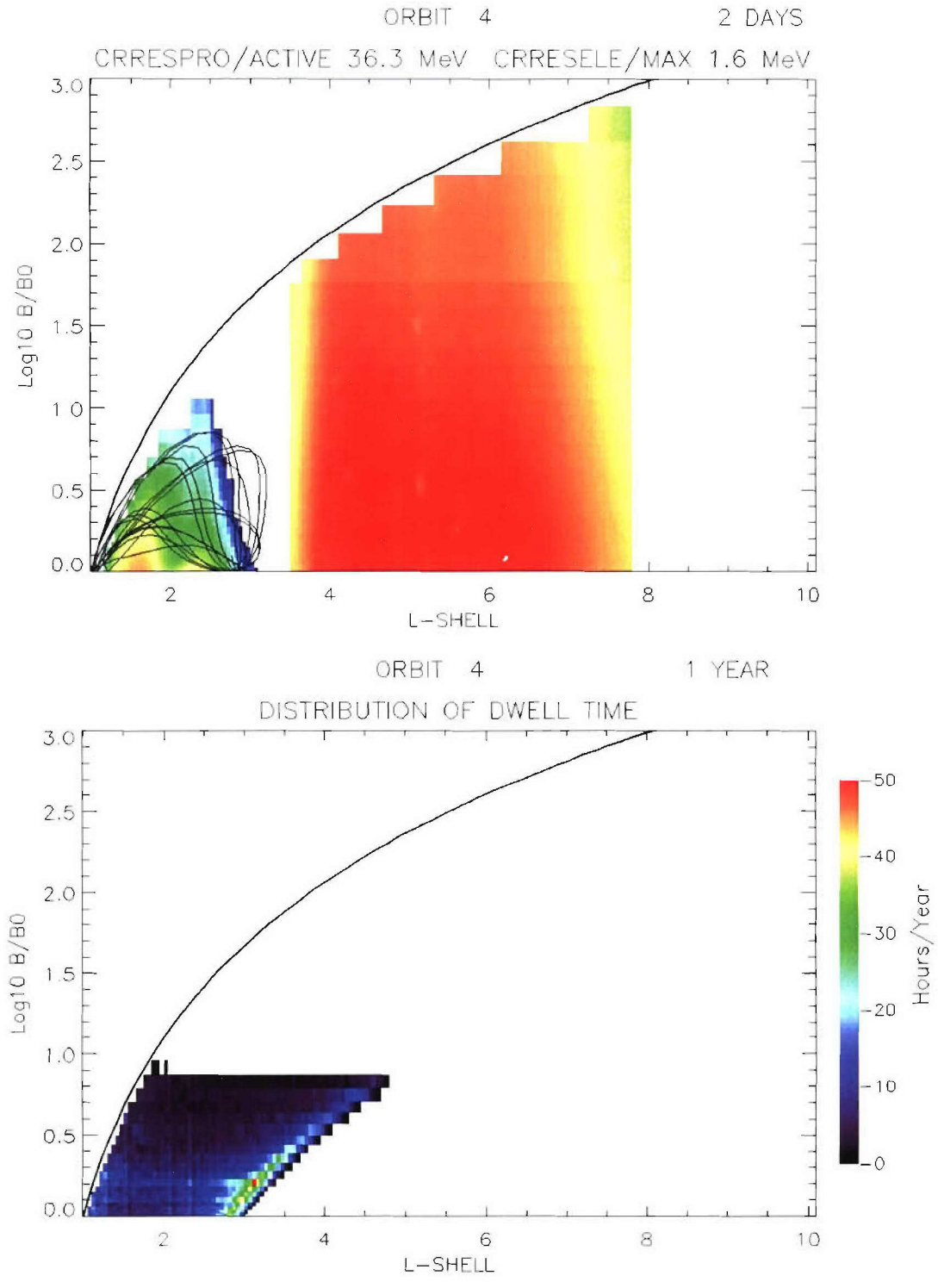

Figure 7. (a) Two Days of Orbit 4 Path (thin solid line) in (L, B/B0) Coordinates Overlayed on the Relative Flux Intensity Distribution of 1.6 MeV Electrons and 36.3 MeV Protons as Determined by the CRRES Models. (b) Dwell Time in (L, B/B0) for a Year's Orbit Path. The thick solid line represents the surface of the Earth.

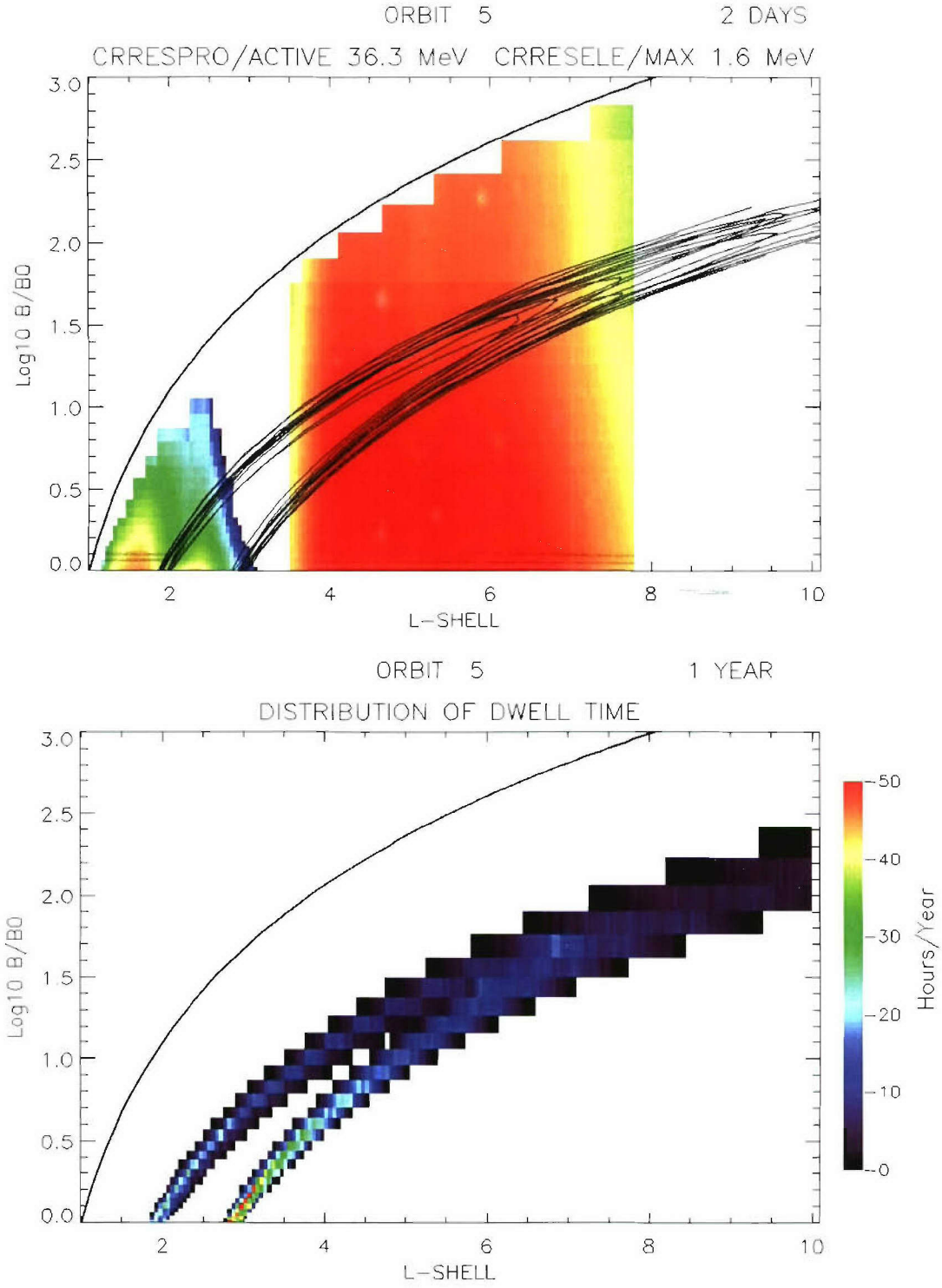

Figure 8. (a) Two days of orbit 5 path (thin solid line) in (L, B/B0) coordinates overlayed on the relative flux intensity distribution of 1.6 MeV electrons and 36.3 MeV protons as determined by the CRRES models. (b) Dwell time in (L, B/B0) for a year's orbit path. The thick solid line represents the surface of the Earth.

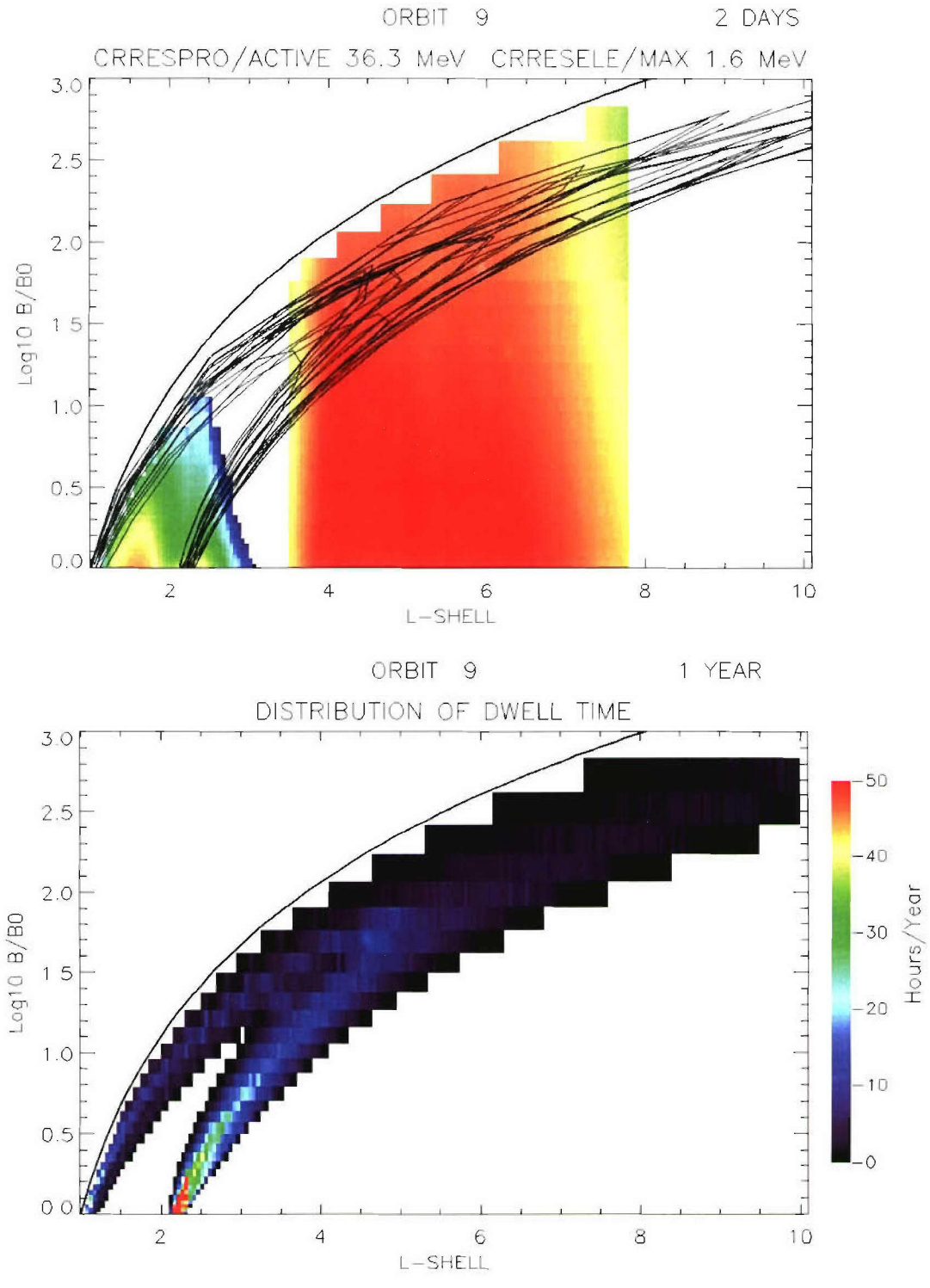

Figure 9. (a) Two days of orbit 9 path (thin solid line) in (L, B/B0) coordinates overlayed on the relative flux intensity distribution of 1.6 MeV electrons and 36.3 MeV protons as determined by the CRRES models. (b) Dwell time in (L, B/B0) for a year's orbit path. The thick solid line represents the surface of the Earth.

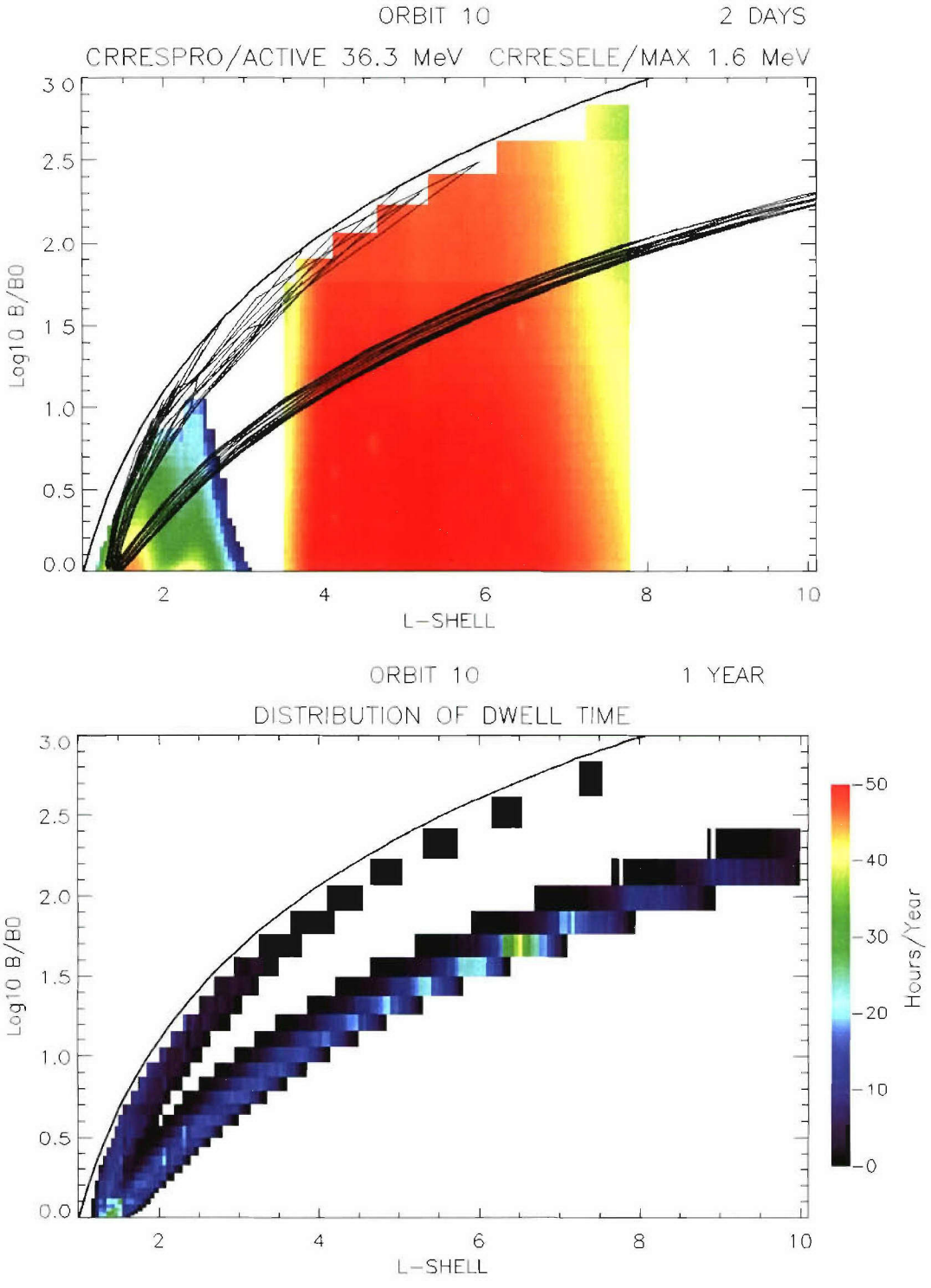

Figure 10. (a) Two days of orbit 10 path (thin solid line) in (L, B/B0) coordinates overlayed on the relative flux intensity distribution of 1.6 MeV electrons and 36.3 MeV protons as determined by the CRRES models. (b) Dwell time in (L, B/B0) for a year's orbit path. The thick solid line represents the surface of the Earth.

The nominal DSX orbit (Figure 6) has good coverage of the MEO slot region from L ~ 1.8 – 3.0 with decreasing equatorial coverage to the edges of the outer zone at L ~ 4.0. As the perigee moves down to 540 km the good coverage region extends down to cover the inner belt (Figure 7). At the higher inclination of 63 degrees the coverage extends to higher L shell but degrades significantly in the equatorial region with gaps in the middle of the slot region (Figure 8) for the 6000 km perigee case (orbit 5). These gaps increase in size as the perigee is decreased through the inner belt. Examining the Magic orbit projections (Figures 9 and 10),we see that a large amount of time is spent at low B/B0 inside L ~ 2.2 with the exact locations of maximum dwell time depending on choice of LTML. A satellite in orbit 10 will spend considerable time in the heart of the inner belt experiencing an intense radiation environment. Both inner belt orbits also clip the horns of the outer zone, acquiring dose from the energetic electrons.

3. RECOMMENDATIONS

The optimum orbit to map the L, B/B0 region relevant to the inner belt orbits while maintaining the capability of DSX to map and carry out experiments in the slot region is orbit 4: 540 km x 12000 km with 28 degrees *or less* inclination. A well-instrumented satellite flying in orbit 4 will be able to map the entire trapped particle inner belt and slot region distributions impacting the inner belt orbit. The energetic electrons in the horns of the outer belt will be missed. However, this population has been much better characterized by existing data sets (e.g. data sets from the Aerospace HEO instruments and the NASA Polar satellite) than have the populations in the inner magnetosphere. Doses for orbit 4 are approximately an order of magnitude higher than the nominal DSX orbit (1) but lower by a factor of approximately two than the worst inner belt orbit considered (10).

Obvious options for implementing orbit 4 in the DSX mission are two: (a) injecting directly into orbit 4, or (b) injecting initially into orbit 1, conducting a year of nominal DSX operations, then moving into orbit 4. The first option has the advantage of immediately obtaining inner belt particle measurements but requires the satellite to be built to a higher dose tolerance than the nominal mission. Option (b) ensures the original DSX mission can be met with the nominal design specifications but delays the gathering of data in the inner belt and carries the risk that the satellite, if not significantly hardened, will not last long enough once moved to the inner belt. Also, the feasibility of including a propulsion system aboard DSX, not included in the nominal mission, must be considered for (b). It is recommend that both option (a) and (b) be fleshed out in terms of cost and schedule impact prior to a decision on whether or not to alter the nominal DSX mission.

REFERENCES

Bell, J.T., M.S. Gussenhoven and E.G. Mullen, Super Storms, *J. Geophys. Res.*, **102**, 14189-14198, 1997.

Brautigam, D.H., M.S. Gussenhoven, and E.G. Mullen, Quasi-static Model of the Outer Zone Electrons, *IEEE Trans. Nucl. Sci.*, **39**, 1797-1803, 1992.

Brautigam, D.H., J. Bell, *CRRESELE Documentation*, PL-TR-95-2128, Phillips Laboratory, Hanscom AFB, MA 10731, 1995. ADA 301770

Gussenhoven, M.S., E.G. Mullen, M.D. Violet, C. Hein, J. Bass, and D. Madden, CRRES High Energy Proton Flux Maps, *IEEE Trans. Nucl. Sci.*, **40**, 1450-1457, 1993.

Gussenhoven, M.S., E.G. Mullen, M. Sperry, K.J. Kerns and J. B. Blake, The Effect of the March 1991 Storm on Accumulated Dose for Selected Satellite Orbits: CRRES Dose Models, *IEEE Trans. Nucl. Sci.*, **39**, 1765-1772, 1992.

Feynman, J., G. Spitale, J. Wang, and S. Gabriel, Interplanetary Proton Fluence Model: JPL 1991, *J. Geophys. Res.*, **98**, 13281-13294, 1993.

Hilmer, R., Ed., *AF-GEOSpace User's Manual Version 2.0 and 2.0P*, update to AFRL-VS-TR-1999-1551 Special Reports, No. 281, available from AFRL (robert.hilmer@hanscom.af.mil), 2001.Also available from NTIS, ADA389056

Kerns, K.J., and M.S. Gussenhoven, *CRRESRAD Documentation*, PL-TR-92-2201, Phillips Laboratory, Hanscom AFB, MA, 1992. ADA 256673

Meffert, J.D., and M.S. Gussenhoven, *CRRESPRO Documentation*, PL-TR-94-2218, Phillips Laboratory, Hanscom AFB, MA, 1994. ADA 284578

Vette, J.I., The NASA/National Space Science Data Center Trapped Radiation Environment Model Program (1964-1991), NSSDC/WDC-A-RS 91-29, available from nssdc.gsfc.nasa.gov, 1991.